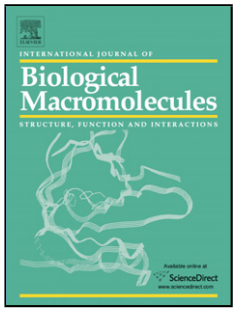

Title: Design, Synthesis and Collagenase Inhibitory Activity of Some Novel Phenylglycine Derivatives as Metalloproteinase inhibitors

Authors: Ankit Ganeshpurkar, Devendra Kumar, Sushil Kumar Singh

PII: S0141-8130(17)32053-6
DOI: https://doi.org/10.1016/j.ijbiomac.2017.10.008
Reference: BIOMAC 8303

To appear in: *International Journal of Biological Macromolecules*

Received date: 7-6-2017
Revised date: 23-9-2017
Accepted date: 3-10-2017

Please cite this article as: Ankit Ganeshpurkar, Devendra Kumar, Sushil Kumar Singh, Design, Synthesis and Collagenase Inhibitory Activity of Some Novel Phenylglycine Derivatives as Metalloproteinase inhibitors, International Journal of Biological Macromolecules https://doi.org/10.1016/j.ijbiomac.2017.10.008

Design, Synthesis and Collagenase Inhibitory Activity of Some Novel Phenylglycine Derivatives as Metalloproteinase inhibitors

Ankit Ganeshpurkar, Devendra Kumar, Sushil Kumar Singh*

Pharmaceutical Chemistry Research Laboratory, Department of Pharmaceutical Engineering & Technology, Indian Institute of Technology (Banaras Hindu University), Varanasi-221005, India.

*Corresponding author. Tel.: +91 542 6702736; fax: + 91 542 368428.
E-mail address: sksingh.phe@iitbhu.ac.in

Abstract

Metalloproteases are a class of proteases having metal ion(s) at their catalytic sites. Bacterial collagenases are involved in human gas gangrene, periodontal diseases, food etc. The Clostridium collagenase occurs in two isoforms COL_G and Col_H. The present work is based on the protein structure-based approach for the development of collagenase inhibitor. The sequence analysis and structural alignment of both isoforms showed significant similarity in active site except aspartate switch present in Col_H. The homology model was developed and validated for Col_H peptidase domain with open aspartate switch followed by the docking of designed ligands. Compound 8b showed better interaction due to the presence of the nitro group. The N-benzyl-arylsulfonyl-phenylglycine derivatives were synthesized and characterized by FT-IR, ^{1}H NMR, ^{13}C NMR and mass spectral analysis. The compounds were evaluated for *C. histolyticum* collagenase inhibitory activity using gelatin-ninhydrin based assay. Compounds 5b, 3b, 11b, 6b and 8b with IC_{50} of 24.34 µM, 29.61µM, 28.39 µM, 31.4 and 32.11 µM respectively were found to be more active. Further, The Ki of most active compound 5b was found to be 22.02µM showing the competitive mode of inhibition of the enzyme. The activity of the derivatives showed correlation with the docking results.

Keywords: *Clostridium histolyticum* collagenase, Phenylglycine, Sulfonamide.

1 Introduction

Metalloproteases (metallopeptidases or metalloproteinases) are a broad class of hydrolases which cleave peptide bonds by the action of a water molecule, achieved by complexing to bivalent metal ions [1]. They belong to a family of 'proteolytic enzymes' termed as endopeptidases. Most of the metalloproteases contain one or two zinc ions in their catalytic site. However, in some cases other metal ions viz. cobalt, nickel, manganese or copper perform the same function. Some enzymes also have two metal ions acting co-catalytically. Metalloproteases have His, Glu, Asp, or Cys residues in various combinations which create a tridentate zinc active site, along with an activated water molecule that completes the coordination sphere of metal ion (Vallee and Auld 1990).

According to the MEROPS database (http://merops.sanger.ac.uk), proteases are classified on the basis of protein structures and their homologies. Metalloproteases are subdivided into 15 clans. The clans MA, MC, MD, ME, MJ, MK, MM, MO and MP require only one catalytic metal ion which is usually zinc ion, other clans i.e. MF, MG, MH, MN and MQ have two metal ions [2]. Clan M- contains all the metalloprotease families which are not yet assigned to a clan. The clan includes enzymes from a wide range of origin such as 'hemorrhagic toxins' from snake venoms, 'collagenases' from higher organisms, and 'thermolysin' from bacteria. It also includes enzymes from 'metzincin family' i.e. serralysin, astacins, adamalysins (ADAMs), and matrixins (matrix metalloproteinase) [3].

Microbial collagenases belong to MEROPS peptidase family M9. This family comprises ofs bacterial metalloproteinases (predicted to be zinc-dependent) obtained from *Vibrio* and *Clostridium* with collagenolytic activity.[4]. The first discovered and commercially available Collagenase was obtained from anaerobic bacterium *Clostridium histolyticum*. It was present as a component of toxic products. Later, other sources like *Achromobacter iophagus* (aerobic

bacterium) and microbes including fungi were also identified. The activity of collagenase is specific on collagen, gelatin and not on other protein substrates [5]. The polypeptide chains of collagen are composed of numerous repeats of a tripeptide amino acid sequence Gly-Pro-X, where X is often a proline, which post-translationally gets converted to hydroxyproline. Collagen degradation takes place during various physiological and pathological conditions. Several reports suggest the role of microbial collagenase in bacterial diseases viz. *Actinobacillus actinomycetemcomitans* in periodontal disease, *Clostridium* species in Necrotizing diseases, pregnancy complications, *Pseudomonas auriginosa* in Emphysema, ecthyma gangrenosum, occular keratitis and pulmonary necrosis.

The structure of clostridial collagenase occurs in four isoforms (Col_G, Col_A, Col_H, and Col_T) [6]. They are multidomain proteins of ~115 kDa of gluzincin superfamily of metalloproteases [7]. The collagenase G (Col_G) and Col_H are obtained from *Clostridium histolyticum*, Col_A from *Clostridium perfringens* whereas as Col_T obtained from *Clostridium tetani*. The Col_G and Col_A have two collagen binding domains (CBDs) and one polycystic kidney disease (PKD) like domain while Col_H, and Col_T have two PKDlike domains but only one CBD [8-10]. The current study aims at the design, synthesis and biological evaluation some novel phenylglycine derivatives as inhibitors of Clostridium Col_G and Col_H (Fig. 1).

2 Experimental section

2.1 Structure-based drug design

2.1.1 Sequence analysis

The sequences of apo forms of *Clostridium* collagenase Col_G and Col_H isoforms were obtained from UniprotKb as fasta file format. The sequence superimposition was carried out using Blastp

(protein-protein BLAST). The analysis was carried out using Blosum 62 scoring matrix with gap cost Existence: 11 Extension: 1 [11, 12].

2.1.2 Structural alignment

The structural alignment of the two proteins were carried out by UCSF chimera matchmaker using Needleman-Wunsch alignment algorithm and Blosum-62 as a scoring matrix. The chain pairing was done by best-aligning pairs of chain between the reference and match structure. The comparison for peptidase domain was performed on Col_G:2Y50 (PDB code) and Col_H:4AR1, CBD s3b of Col_G:4HPK and s3 of Col_H:3JQW, and PKD s2 of Col_G:4AQO and s2a of Col_H:4U6T [13].

2.1.3 Structural refinement

The structural refinement of PDB 2Y50 of Col_G was carried out by Modeller 9.18 using UCSF Chimera interface. The KSDSSP (Kabsch and Sander Define Secondary Structure of Proteins) algorithm with the parameters: energy cutoff -0.5, minimum helix length 3, minimum strand length 3 was used which was followed by structural analysis by the matchmaker module. Further, Dockperp was used to add charges, hydrogens and remove water molecules from the pdb [14]. The incomplete side chains were added by using Dunbrack rotamer library [15]. This was followed by running PDB2PQR - a Python-based structural conversion utility to assign charge and protonated state to various residues at pH 7.0 using Amber force field [16].

2.1.4 Homology modeling

Three-Dimensional structure of open conformation of peptidase domain of the Col_H was constructed by homology modeling using SWISS-MODEL accessible via the ExPASy web server [17]. The quality of the models was evaluated using the RAMPAGE [18], PROCHECK [19],

ERRAT [20], Verify 3D [21], GMQE [17], QMEANDisco and QMEAN [22]. Visualization of the model was done with Chimera. The tertiary structure of Col_H peptidase having active conformation was deposited to the Protein Model DataBase (PMDB). PM0081035 was assigned to be the identifier for the structure. The Model was refined using Dockprep and PDB2PQR utility [23].

2.1.5 Preparation of Proteins and Ligands

The structurally refined protein pdb files were converted to pdbqt files using grid module of autodock tools 1.5.6. The +2 charge was assigned to the zinc ions of the proteins manually. The ligands were sketched using Chemdraw 16 and their energies were minimized using MM2 of Chem3D. The ligands were then saved as pdb files. These pdb files were converted to pdbqt using ligand preparation module of autodock tools 1.5.6.

2.1.6 Grid Generation

The autogrid 4.0 was used to calculate grid maps of interaction energies with various atom types present in the ligands (A, C, HD, NA, N, OA, S, Br, Cl and I). The grid size was set to 52 × 48 × 52 and 52 x 44 x 42 xyz points respectively for Col_G (PDB id-2Y50) and Col_H(PM0081035) with a grid spacing of 0.375 Å. The grid center was placed at coordinates (x, y, and z) -26.587, -6.178, -15.805 for Col_G and -28.572 -3.727 -14.247 for Col_H.

2.1.7 Docking

The docking was performed by Autodock 4.0 using Lamarckian Genetic Algorithm(LGA). It estimated the free binding energy of ligand-receptor complex for scoring various conformations. The docking was performed using algorithm with 10 runs, 150 population size, 2,500,000 maximum number of energy evaluations and 27,000 maximum number of generations. It used

'semiempirical free energy force field' to evaluate conformations at the time of docking simulations. The Docked structure was visualized by using Discovery Studio 2016 for obtaining the binding interactions [24, 25].

2.2 Synthesis of *N-benzyl-arylsulfonyl-phenylglycine*.

All the chemicals and solvents were of analytical grade or purified by standard methods before use. These were purchased from Avra (Hyderabad), Spectrochem, S.D. Fine (Mumbai) and Sigma-Aldrich (U.S.A.). The reactions were monitored by thin-layer chromatographic (stationary phase: florescent F254 containing silica gel 60 G coated on aluminum sheets; mobile phase: 40% ethyl acetate in hexane). The melting point values were determined by an open capillary method using BARNSTEAD/Electrothermal/Stuart-SMP10 melting point apparatus and are uncorrected. Fourier Transform-Infra red (FT-IR) spectra in powder form, were recorded on Shimadzu FTIR-8400s. ^{1}H NMR (500 MHz) and ^{13}C NMR (125 MHz) spectra were obtained on a BRUKER 500 FT-NMR spectrometer. Chemical shift values are reported in parts per million (ppm) downfield from tetramethyl silane (TMS) used as an internal reference standard, and coupling constants (J) were given in Hz. Mass spectra were recorded using Waters Q-TOF Micromass (ESI-MS).

2.2.1 General procedure for the synthesis of *N- aryl sulfonyl-phenyl glycine*. (1a-12a)

An amount of 1.0 g (6.6 mmol) of phenyl glycine and stoichiometric amount (15 mmol) of the base (Na_2CO_3/K_2CO_3) dissolved in acetone and water mixture (70 mL:25 mL). Different substituted aryl sulfonyl chloride(6.7 mmol) dissolved in acetone was added in a dropwise to the reaction mixture. The reaction mixture was stirred at room temperature for 4–10 hrs and completion of reaction was monitored by TLC . The solvent was evaporated *in vacuo*; the reaction mixture was taken in 100 mL of distilled water and the crude product was precipitated by addition

of dil. HCl. The precipitate was filtered off and dried at room temperature in desiccator [26]. The precipitate was recrystallized using the warm water-methanol mixture to yield pure compound.

2.2.2 General procedure for the synthesis of N-*benzyl-arylsulfonyl-phenylglycine.* (1b-12b)

N-aryl sulfonyl-phenyl glycine (5 mmol) and stoichiometric amount of benzyl chloride were suspended/dissolved in 50 mL of anhydrous acetonitrile, and stoichiometric amount of triethylamine (5 mmol, 0.71 mL) was added to it. The reaction mixture was refluxed for 24-48hrs on water bath and monitored by TLC. The solvent was evaporated *in vacuo* after the completion of the reaction. The reaction mixture obtained was taken in 50 mL of water; the pH was brought to 7 with citric acid and the crude carboxylic acids 91b-12b) were extracted with ethyl acetate. The ethyl acetate layer was dried over anhydrous Na_2SO_4 and solvent was evaporated *in vacuo* to obtain crude product. The residue obtained after removal of ethyl acetate was purified by column chromatography through stepwise gradient elution with ethyl acetate in hexane (max 10%) to get final product (Fig. 2).

2.3 Collagenase inhibition assay

2.3.1 Requirements

- **Reaction buffer:** Reaction buffer was composed of 50 mM Tris-HCl, pH 7.5, 5 mM $CaCl_2$, and 1 µM $ZnCl_2$.
- **Ninhydrin reagent:** In brief, 80 mg of $SnCl_2{\cdot}2H_2O$ was dissolved in 50 mL of citrate buffer (0.2 M, pH 5.0) and purged with N_2. Ninhydrin solution was prepared by dissolving 0.5 g of ninhydrin in 10 mL of DMSO. The ninhydrin reagent for color development, was made by mixing the $SnCl_2$ solution with an equal volume of ninhydrin solution before use.

- Gelatin (660 µg of gelatin was dissolved in 343 µL reaction buffer) and *Clostridium* collagenase IV (Himedia, Mumbai) used in the assay was prepared by dilution with reaction buffer to the desired concentration.
- **Quenching buffer**: Quenching buffer contained 12% (w/v) PEG 6000 and 25 mM EDTA.

2.3.2 Procedure

The assay was performed by incubating 3.5 µL of various concentrations of inhibitor (2.5-100µM) with a solution of 7 µL collagenase (1 mg/mL) and equilibration for 5 min before initiation of the digestion reaction. The digestion reaction was conducted at 37 °C with addition of gelatin solution. After 10 min, an equal volume of quenching buffer was added to cease the reaction. The glycine liberated was estimated by adding 500 µL of ninhydrin reagent to the above reaction mixture in an Eppendorf tube (cap closed) which was heated at 80 °C for 10 min in a water bath. Once the tubes were cooled, an additional 500 µL double distilled H_2O was added and mixed well. Amino acids (or peptides) resulting from gelatin hydrolyzation were detected on Biotek multimode microplate reader at 570nm against blank. The reaction mixture except inhibitor was used as control. A sample containing only ninhydrin, without gelatin and collagenase, of the same volume of reaction buffer was used as blank. 1,10-phenanthroline a transition metal chelator was used as standard inhibitor. The percentage inhibitions of *Clostridia* collagenase activity of the compounds were calculated assuming that the control sample has 100% activity. IC_{50} values were calculated for each sample by plotting log inhibitor dose and normalized response (by variable slope method) and expressed as the mean ± SEM of three independent measurements (Graphpad Prism 5) [27].

2.4 Determination of Ki

The enzyme kinetics was determined for clostridial collagenase using the similar protocol in the presence of different concentrations of substrate i.e. gelatin (0.107, 0.314, 0.628, 1.25, 1.886, 2.5 mg/ml) with and without 5b. Lineweaver–Burk plot was used to determine the kinetic mechanism.

3 Results and Discussion

3.1 Structure-based drug design

3.1.1 Sequence analysis

A pairwise amino acid sequence comparison of the collagenase Col_G and Col_H isoform of *C. histolyticum* using BLASTP 2.6.1+ showed 43% identical residues and similarity of 60% with 89% of query cover. The sequence comparison of their peptidase domain showed 49% similarity for query cover of 98%. These are large multidomain protein with mol. wt. ~115 kDa. They have 'polycystic kidney disease (PKD)-like domain', 'Collagen binding domain (CBDs)' apart from peptidase and activator domains. The peptidase domain of Col_G extends from D398-G790 and Col_H from D330-G721. The mol. wt. of this subunit is ~44.5kDa and consists of Zinc ion on its catalytic site. They zinc binding motif HEXXH is common among these enzymes with additional glutamate residue located after 28 amino acids. Thus indicating their homology with gluzincin clan of peptidase. The two CBDs present in Col_G extend from T885-I999 and N1004-1118 while the only CBD of Col_H extends from Y903-R1021. The Col_G has only one PKD extending from N795-N880 while Col_H has two PKDs i.e. from N725-D810 and N814-D900. The Sequence alignment of Col_G s2 and Col_H s2a showed 51% identical, 62% positive residues for 100% query cover (supplementary).

3.1.2 Structural alignment

The BLOSUM-62 scoring matrix of the Needleman-Wunsch algorithm was used to align protein using UCSF Chimera. The structural superimposition between Col_G (PDB id- 2Y50) and Col_H (PDB id- 4AR1) peptidase domains have RMSD of 0.880 Å between 309 pruned atom pairs of all 379 pairs. The zinc ion which is surrounded by zinc ligands has the same position about space in both the isoforms in spite of low sequence similarity. The RMSD of the three zinc ligands of Col_G and Col_H between H-523 vs. H-455, H-527 vs. H-559 and E-555 vs. E-487 are 0.662, 0.203 and 0.428 respectively quite below the complete structure RMSD. Further, the Col_G:E-524 and Col_H:N-421 stabilizes their respective zinc ions which are quite apart from each other. The alanine side chain (Col_G:A-555 and Col_H:A-490) forms hydrophobic base of the active site cavity ~ 4 Å below the zinc with RMSD 0.732. The fringe strand is composed of hydrophobic residues (G-493 to E-498) of the five stranded β-sheets line the S1` pocket. This site of Col_G is lined by conserved G-493, G-494 residues forming oxyanion hole like structure which holds the carbonyl oxygen of P1` residue. These residues are also conserved in Col_H (G-425 to E-430) except M-427 with a RMSD 1.256.

The RMSD between Col_G:S-489 and Col_H:D-421 is 10.071 where D-421 of Col_H forms ionic interaction with zinc ion. This interaction leads to proximal placement of segment D-414 to D-424 near zinc in Col_H. The ligand binding displaces its location and adopts similar conformation as that of Col_G (Aspartate Switch).

The s3b and s3 (CBD) of Col_G and Col_H adopt similar ‘β-sandwich jelly roll’ conformation having nine β-strands. The RMSD between 92 pruned atom pairs is 0.771 Å across all 108 pairs. The literature also suggests a high degree of similarity with Cα-RMSD of 1.4 Å in spite of low sequence similarity. The coordination residues of the two calcium atoms are also nearly similar in

both isoforms of this CBD except Col_G:ASP 904 and Col_H:ASN 873 having RMSD of 0.276. The PKD domain of both Collagenase have RMSD between 82 pruned atom pairs is 0.745 Å across all 86 pairs (Fig. 3).

3.1.3 Structural refinement

The PDB 2Y50 was refined by modeller and had RMSD 0.049Å over the actual PDB with no addition of side chain thus indicating good quality of the model. Further, the dockprep removed all the additional heteroatoms from the PDB, added hydrogen atom, assigned protonation state to H, D, E, K, C and total charge of -10.00 using charge model AMBER ff14SB. The PDB2PQR added +2 charge on the Zinc ion using Gasteiger method.

3.1.4 Homology modeling

A three-dimensional structure of Col_H collagenase peptidase domain in open conformation was developed using SWISS-MODELbased on the template of *C. histolyticum* collagenase (Col_G) in apo form (PDB code 2Y50). The selected model was validated using RAMPAGE (Ramachandran Plot analysis) and PROCHECK (overall stereochemical property).

The VERIFY_3D score for the model showed 94.59% of the residues had an average 3D-1D score ≥ 0.2 which was far above the cutoff limit of 80%. The Ramachandran plot analysis of the model by RAMPAGE and PROCHECK server showed a good quality of model having more than 90% of residues in the most favoured region (Table 1). The overall quality factor determined by ERRAT was found to 94.96 indicating good high-resolution structure.

The GMQE shows expected accuracy of a model built with that alignment and template. The GMQE Score for the model was 0.81 indicating the nearness of the model to the template. The previous literature report also suggested that ligand binding to the catalytic zinc displaced the

aspartate switch acquiring conformation of Col_G(template) [28]. The QMEAN of the model is -0.90 which is the estimation of both global and local quality of model with reference to X-ray crystallography structures. It is based upon pairwise distance-dependent potential of all-atom and Cβ interactions, torsion angle potential, and solvation potential. The Cβ interactions and torsion angle potential are not favorable for the model. Further, QMEANDisCo method showed the local quality of protein where all the active site residues have good local quality scores. Thus, most of the validation parameters indicated confidence over the developed model of Col_H peptidase domain.

The model was further processed for docking using Dockprep and PDB2PQR. The hydrogen was and -4.0 charge was added using AMBER ff14SB and +2 charge was assigned to Zinc ion using gasteiger method. The developed model had free Asp 421 residues when compared with actual conformation of Col_H found in nature i.e. Asp 421 coordinated with Zinc ion. The ligand, when bound to active site, displaced the Asp 421 and occupied the site. The model developed also mimicked the open conformation of enzyme which would be suitable for docking study (Fig. 4).

3.1.5 Grid Generation and Docking

The grid covering the catalytic zinc ion and various pockets was developed for different ligand atom types along with receptor desolvation map and was used for docking calculation. The docking was performed using LGA. The best conformation was selected with highest binding energy after the docking search was completed. The interactions between protein and ligand conformations, including hydrogen bonds and the bond lengths, were analyzed. The compounds were designed to bind with zinc as well as to provide extra interactions with the side pockets for selectivity over other metalloproteinase. Docking study showed the interaction of COOH group with catalytic Zn ion in both isoforms. The introduction of the sulfonamide group showed interaction with S1` pocket of the

enzyme. This group showed hydrogen bonding interactions with the G-337, G-378(Col_G) of S1` pocket in some of the ligand viz. 3b, 5b, and 9b. The inhibitors also showed interaction with Col_H S1` pocket (G-98, G-99) i.e. 3b, 4b, 6b, 7b, 8b, 9b (Table 2 & 3). The designed inhibitors also showed interaction with E-408 (Col_G) and E-129 (Col_H) which is part of HEXXH motif. The nitro compound 5b also showed some extra interactions in both isoforms (Fig. 5).

3.2 Synthesis and Characterization of Compounds

The synthesis of N-aryl-sulfonyl derivatives was initiated by nucleophilic attack of amine (Phenyl glycine) on sulfonyl group of different aryl sulfonyl chloride leading to release of chloride. The HCl formed may protonate amine group causing a decrease in reaction rate. Hence, inorganic bases (Na_2CO_3 / K_2CO_3) were added. The product formed in the first step was precipitated out in acidic condition (pH 2) yielding white fine needle shape crystals. The next step followed a nucleophilic attack of nitrogen of sulfonamide group (acidic in nature) on the benzyl chloride. The HCl formed was neutralized by addition of TEA. The reaction was carried out in acetonitrile, a polar aprotic solvent. The final synthesized compounds(**1b-12b**) were purified by column chromatography using silica gel. The stepwise gradient elution using ethyl acetate in hexane facilitated the separation process.

The percentage yield of most of the compounds was good except the nitro bearing compounds. The melting point range, R_f value and solubility were determined. The melting point range of the final compounds (1b-12b) was found to be in the range of 100-145˚C with *para*-nitro derivative having the highest melting point which may be due to inter-molecular hydrogen bonding. The R_f value of the compounds (1b-12b) were nearly halfway of the solvent front except for nitro and N-acetamide derivatives. These compounds had low R_f value due to their high polarity. The FT-IR spectra of all the compounds (1b-12b) showed a characteristic carboxylic OH peak in the range of

3400-2400 cm^{-1}, C-H stretching around 3000 cm^{-1}, carbonyl peak of carboxylic acid around 1730-1700 cm^{-1}, strong sulfonamide peak around 1375-1300 cm^{-1}, and 1350-1140 cm^{-1}. A peculiar peak of nitro (N=O) was found around 1550 and 1350cm^{-1} in the nitro group-bearing compounds. The ^{1}H NMR of final compounds showed singlet around δ value 9 ppm showing proton of a carboxylic acid, a deviation from normal range, between 11-12 ppm. This may be due to stearic hindrance which made it highly shielded [29]. Aromatic protons with multiplet splittings were observed between 8.3-7.l. The chiral proton of phenyl glycine and benzylic proton appeared between 5.5-4.9 ppm. The splitting of benzylic CH_2 proton signal was observed at 500 MHz. ^{13}C spectra also showed C=O around 169 ppm, aromatic carbon around 145-120 ppm, benzylic carbon near 65 ppm and chiral tertiary carbon around 59 ppm. The mass spectra of the compounds showed a base peak at M^+ and M^++1 which corresponding to their observed molecular weight. The chlorine and bromo bearing compounds (4b, 3b) displayed two peaks at $M^+$and $(M+2)^+$ peak (percentage abundance ratio: 3:1 and 1:1) corresponding to the isotopes of chlorine and bromine respectively.

Spectral data

3.2.1 *2-(N-benzyl-N-tosylamino)-2-phenylacetic acid* (1b)

FT-IR (KBr disc, cm^{-1}): 3286.81 (-OH), 2960.83(C-H sym. streching), 1735.99 (-C=O-), 1330.93, 1159.26 (-SO_2NH-), 1091.09(S=O). ^{1}H NMR (500 MHz, DMSO-d_6) δ(ppm): 8.89-8.87 (s,1H, COOH), 7.61-7.13 (m, 14H, Ar-H), 4.98-4.96 (s, 1H, C-H), 4.92-4.90 (d, 2H, -CH_2-), 2.32 (s, 3H, -CH3). ^{13}C NMR (125 MHz, DMSO-d_6) δ(ppm): 169.54(C=O), 142.60-126.5 (Aromatic carbon), 66.36(-CH-), 59.456(-CH2), 20.95(-CH_3). (ESI) m/z $[M + H]^+$ for $C_{22}H_{21}NO_4S$ predicted 395.47 , measured 396.89.

3.2.2 *2-(N-benzylphenylsulfonamido)-2-phenylacetic acid* (2b)

FT-IR (KBr disc, cm^{-1}): 3290.81 (-OH), 2965.23(C-H sym. streching), 1725.96 (-C=O-), 1332.93, 1155.26 (-SO_2NH-), 1092.19(S=O). ^{1}H NMR (500 MHz, DMSO-d_6) δ(ppm): 8.98-8.96 (s,1H, COOH), 7.71-7.14 (m, 15H, Ar-H), 5.11-5.10 (s, 1H, C-H), 4.99-4.90 (d, 2H, -CH_2-). ^{13}C NMR (125 MHz, DMSO-d_6) δ(ppm): 169.54(C=O), 142.60-126.5 (Aromatic carbon), 66.36(-CH-), 59.456(-CH_2-). (ESI) m/z $[M + H]^+$ for $C_{21}H_{19}NO_4S$ predicted 381.10, measured 382.3.

3.2.3 *2-((N-benzyl-4-bromophenyl)sulfonamido)-2-phenylacetic acid* (3b)

FT-IR (KBr disc, cm^{-1}): 3283.81 (-OH), 2961.83(C-H sym. streching), 1722.35 (-C=O-), 1350.93, 1156.06 (-SO_2NH-), 1091.09(S=O). ^{1}H NMR (500 MHz, DMSO-d_6) δ(ppm): 9.09-9.07 (s,1H, COOH), 7.70-7.13 (m, 14H, Ar-H), 5.15-5.13 (s, 1H, C-H), 5.03-4.94 (d, 2H, -CH_2-). ^{13}C NMR (125 MHz, DMSO-d_6) δ(ppm): 169.37(C=O), 139.74-127.42 (Aromatic carbon), 66.45(-CH-), 59.45 (-CH_2-). (ESI) m/z $[M + H]^+$ for $C_{21}H_{18}BrNO_4S$ predicted 460.34, measured 461.05.

3.2.4 *2-((N-benzyl-4-chlorophenyl)sulfonamido)-2-phenylacetic acid* (4b)

FT-IR (KBr disc, cm^{-1}): 3294.81 (-OH), 2969.22(C-H sym. streching), 1735.99 (-C=O-), 1330.93, 1134.26 (-SO_2NH-), 1051.59(S=O). ^{1}H NMR (500 MHz, DMSO-d_6) δ(ppm): 9.08 (s,1H, COOH), 7.63-7.13 (m, 14H, Ar-H), 5.14 (s, 1H, C-H), 5.03-4.94 (d, 2H, -CH_2-). ^{13}C NMR (125 MHz, DMSO-d_6) δ(ppm): 169.39(C=O), 140.15-126.17 (Aromatic carbon), 66.47(-CH-), 59.46 (-CH_2-). (ESI) m/z $[M + H]^+$ for $C_{21}H_{18}ClNO_4S$ predicted 415.89, measured 416.85.

3.2.5 *2-((N-benzyl-4-nitrophenyl)sulfonamido)-2-phenylacetic acid* (5b)

FT-IR (KBr disc, cm^{-1}): 3275.34 (-OH), 2976.26 (C-H sym. streching), 1720.56 (-C=O-), 1525.74 (NO_2 assym strech.) 1350.22, 1170.83 (-SO_2NH-), 1087.89(S=O). ^{1}H NMR (500 MHz, DMSO-d_6) δ(ppm): 9.36-9.34 (s,1H, COOH), 8.21-7.13 (m, 14H, Ar-H), 5.24-5.22 (s, 1H, C-H), 5.03-4.95

(d, 2H, -CH_2-). ^{13}C NMR (125 MHz, DMSO-d_6) δ(ppm): 169.23 (C=O), 149.25-124.04 (Aromatic carbon), 66.54 (-CH-), 59.48 (-CH_2-). (ESI) m/z $[M + H]^+$ for $C_{21}H_{18}N_2O_6S$ predicted 426.44, measured 427.56.

3.2.6 *2-((N-benzyl-4-(N-acetamido)phenyl)sulfonamido)-2-phenylacetic acid* (6b)

FT-IR (KBr disc, cm^{-1}): 3277.81 (-OH), 2950.23(C-H sym. streching), 1736.29 (-C=O-), 1332.22, 1159.26 (-SO_2NH-), 1090.09(S=O). ^{1}H NMR (500 MHz, DMSO-d_6) δ(ppm): 10.26(s, 1H, -NH-), 9.35-9.33 (s,1H, COOH), 8.21-7.13 (m, 14H, Ar-H), 5.23-5.21 (s, 1H, C-H), 5.02-4.94 (d, 2H, -CH_2-), 2.11(s, 3H, CH_3-CO). ^{13}C NMR (125 MHz, DMSO-d_6) δ(ppm): 169.23 (C=O), 154.43 (C=O), 149.25-124.04 (Aromatic carbon), 66.54 (-CH-), 59.48 (-CH_2-), 23.85(-CH_3). (ESI) m/z $[M + H]^+$ for $C_{23}H_{22}N_2O_5S$ predicted 438.49, measured 439.52.

3.2.7 *2-((N-benzyl-2-methylphenyl)sulfonamido)-2-phenylacetic acid* (7b)

FT-IR (KBr disc, cm^{-1}): 3296.81 (-OH), 2970.43(C-H sym. streching), 1725.69 (-C=O-), 1332.26, 1159.26 (-SO_2NH-), 1031.39(S=O). ^{1}H NMR (500 MHz, DMSO-d_6) δ(ppm): 8.97-8.95 (s,1H, COOH), 7.71-7.12 (m, 14H, Ar-H), 5.11-5.10 (s, 1H, C-H), 4.99-4.90 (d, 2H, -CH_2-), 2.62 (s, 3H, -CH_3). ^{13}C NMR (125 MHz, DMSO-d_6) δ(ppm): 169.34(C=O), 142.70-127.5 (Aromatic carbon), 66.77 (-CH-), 59.46(-CH_2-), 21.33(-CH_3). (ESI) m/z $[M + H]^+$ for $C_{22}H_{21}NO_4S$ predicted 395.47 , measured 396.78.

3.2.8 *2-((N-benzyl-3-nitrophenyl)sulfonamido)-2-phenylacetic acid* (8b)

FT-IR (KBr disc, cm^{-1}): 3316.81 (-OH), 2942.83(C-H sym. streching), 1731.69 (-C=O-), 1331.23, 1154.26 (-SO_2NH-), 1061.19(S=O). ^{1}H NMR (500 MHz, DMSO-d_6) δ(ppm): 9.35-9.33 (s,1H, COOH), 8.23-7.13 (m, 14H, Ar-H), 5.23-5.21 (s, 1H, C-H), 5.02-4.96 (d, 2H, -CH_2-). ^{13}C NMR

(125 MHz, DMSO-d_6) δ(ppm): 169.43 (C=O), 148.25-124.04 (Aromatic carbon), 66.24 (-CH-), 59.38 (-CH_2-). (ESI) m/z $[M + H]^+$ for $C_{21}H_{18}N_2O_6S$ predicted 426.44, measured 427.37.

3.2.9 *2-((N-benzyl-2-nitrophenyl)sulfonamido)-2-phenylacetic acid* (9b)

FT-IR (KBr disc, cm^{-1}): 3276.81 (-OH), 2930.23(C-H sym. streching), 1725.39 (-C=O-), 1331.93, 1157.26 (-SO_2NH-), 1055.29(S=O). ^{1}H NMR (500 MHz, DMSO-d_6) δ(ppm): 9.37-9.34 (s,1H, COOH), 8.29-7.15 (m, 12H, Ar-H), 5.24-5.22 (s, 1H, C-H), 5.06-4.96 (d, 2H, -CH_2-). ^{13}C NMR (125 MHz, DMSO-d_6) δ(ppm): 169.73 (C=O), 148.95-124.23 (Aromatic carbon), 66.26 (-CH-), 59.28 (-CH_2-). (ESI) m/z $[M + H]^+$ for $C_{21}H_{18}N_2O_6S$ predicted 426.44, measured 427.62.

3.2.10 *2-((N-benzyl-(2,4,6-triisopropyl)-phenylsulfonamido)-2-phenylacetic acid* (10b)

FT-IR (KBr disc, cm^{-1}): 3282.95 (-OH), 2960.80, (C-H sym. streching), 1728.28 (-C=O-), 1332.86, 1151.54 (-SO_2NH-). ^{1}H NMR (500 MHz, DMSO-d6) δ(ppm): 8.97-8.95 (s,1H, COOH), 7.71-7.12 (m, 12H, Ar-H), 5.11-5.10 (s, 1H, C-H), 4.99-4.90 (d, 2H, -CH_2-), 2.77-2.79 (m, 3H, -CH-), 1.26-1.21 (m, 18H, -CH_3). ^{13}C NMR (125 MHz, DMSO-d6) δ(ppm): 168.34(C=O), 142.50-127.5 (Aromatic carbon), 66.77 (-CH-), 59.46(-CH_2-), 34.42, 30.11(-CH-), 22.33, 24.12(-CH_3). (ESI) m/z $[M + H]^+$ for $C_{30}H_{37}NO_4S$ predicted 507.69, measured 508.39.

3.2.11 *2-((N-benzyl-4-Iodophenyl)sulfonamido)-2-phenylacetic acid* (11b)

FT-IR (KBr disc, cm^{-1}): 3273.31 (-OH), 2972.4 (C-H sym. streching), 1724.42 (-C=O-), 1336.71, 1163.11 (-SO_2NH-). ^{1}H NMR (500 MHz, DMSO-d_6) δ(ppm): 9.12 (s,1H, COOH), 7.62-7.13 (m, 14H, Ar-H), 5.13 (s, 1H, C-H), 5.03-4.95 (d, 2H, -CH_2-). ^{13}C NMR (125 MHz, DMSO-d_6) δ(ppm): 169.19(C=O), 141.25-126.17 (Aromatic carbon), 66.42(-CH-), 59.36 (-CH_2-). (ESI) m/z $[M + H]^+$ for $C_{21}H_{18}INO_4S$ predicted 507.34, measured 508.48.

3.2.12 *2-((N-benzyl-4-(tertbutyl)phenyl)sulfonamido)-2-phenylacetic acid* (12b)

FT-IR (KBr disc, cm^{-1}): 3259.81 (-OH), 2964.69 (C-H sym. streching), 1745.64 (-C=O-), 1332.86, 1153.87 (-SO_2NH-), 1087.89(S=O). ^{1}H NMR (500 MHz, DMSO-d_6) δ(ppm): 9.01 (s,1H, COOH), 7.58-7.15 (m, 14H, Ar-H), 5.13 (s, 1H, C-H), 4.99-4.90 (d, 2H, -CH_2-), 1.34(s, 9H, -CH_3). ^{13}C NMR (125 MHz, DMSO-d_6) δ(ppm): 169.19(C=O), 141.25-126.17 (Aromatic carbon), 66.42(-CH-), 59.36 (-CH_2-), 38.54(C), 29.43(CH_3). (ESI) m/z $[M + H]^+$ for $C_{25}H_{27}NO_4S$ predicted 437.55, measured 438.59.

3.3 Collagenase inhibition assay

The assay is based on the principle that collagenase breaks down gelatin (substrate) to produce free amino acids. The free amino acid (glycine) produced react with ninhydrin at 80˚C to produce violet colour. The intensity of colour developed is directly dependent on the concentration of free amino acids in the reaction mixture, which could be determined by spectrophotometric analysis at 570 nm. [27]. 5b, 3b, 11b, 6b, and 8b were found to be more active with IC_{50} values of 24.34 µM, 29.61µM, 28.39 µM, 31.4 and 32.11 µM respectively. The other derivatives also had similar activity with an IC_{50} in the range of 30-70 µM. The *para*-nitro, *para*-N-acetamido as well as *para*-chloro derivatives, were found to be more potent than *para*-alkyl derivatives. The carboxyl group may serve as zinc binding group anchoring the molecule at the active site. The sulfonamide group was introduced in P1` part of the compounds with the idea that the sulfonyl group may provide some extra interaction with S1` pocket of the enzyme. The docking study also showed the possible interaction with the S1` pocket residues. The *para*-nitro and *para*-N-acetamido derivatives were active due to some extra hydrogen bonding interaction with the S1`-side pocket. The decreased binding affinity of *para*-alkyl derivatives may be due to their inability to have more hydrogen bonding interactions. The *para*-Chloro derivatives may be active due to some additional vander

waal's interaction with the surface of the enzyme. The introduction of benzyl group may provide some additional weak interactions with the S1 pocket of the enzyme (Table 4).

3.4 Determination of Ki

The Lineweaver-Burk plot had shown the competitive type of inhibition of the enzyme by 5b. The results suggest that designed inhibitor may have occupied active site of the enzyme. The Ki of 5b was calculated using the formula:

$$Ki = \frac{Km \times (IC50)}{(Km_{App} - Km)}$$

where Km, Km_{app} was obtained for X intercept of the plot. The Ki of 5b was found to be 22.02µM. It may be extrapolated from the study that the designed inhibitor may have shown affinity toward zinc present in the active site as the velocity of the hydrolysis of gelatin decreased with increase in inhibitors concentration.

4 Conclusion

In the present study, a series of compounds were designed for metalloproteinase inhibition and provided initial hits. Their further refinement and optimization may provide a lead. This study used structure based drug design technique that identified the amino acids involved in interaction with the phenylglycine derivatives. In *Clostridium* collagenase inhibition assay, the compounds followed the order: 5b>11b>3b>6b>8b>9b>7b>4b>2b>1b>12b>10b. The potent compounds 5b, 3b, 11b, 6b, and 8b, were found to be more active with IC_{50} of 24.34 µM, 29.61µM, 28.39 µM, 31.4 and 32.11 µM respectively. The study highlights the importance of a zinc binding group for the metalloproteinase inhibitors and also sheds light on the preference of the side chains (sulfonyl

group) for effective backbone binding to the enzyme for proper inhibition. The designed series can further be tested on MMPs which share structural similarity with bacterial collagenase.

Acknowledgment

Authors immensely thank research support grant from the Department of Biotechnology (DBT), New Delhi, India (File No. BT/PR9624/MED/30/1253/2013 dated-29/11/2014) and SAIF/CIL, Punjab University, Chandigarh for providing mass spectra.

References

[1] J. Mansfeld, Metalloproteases, in: J. Polaina, A.P. MacCabe (Eds.), Industrial Enzymes: Structure, Function and Applications, Springer Netherlands, Dordrecht, 2007, pp. 221-242.
[2] N.D. Rawlings, M. Waller, A.J. Barrett, A. Bateman, MEROPS: the database of proteolytic enzymes, their substrates and inhibitors, Nucleic Acids Res 42(Database issue) (2014) 23.
[3] J. Huxley-Jones, T.-K. Clarke, C. Beck, G. Toubaris, D.L. Robertson, R.P. Boot-Handford, The evolution of the vertebrate metzincins; insights from Ciona intestinalis and Danio rerio, BMC evolutionary biology 7(1) (2007) 1.
[4] N.D. Rawlings, A.J. Barrett, A. Bateman, MEROPS: the database of proteolytic enzymes, their substrates and inhibitors, Nucleic acids research 40(Database-Issue) (2012) 343-350.
[5] M.B. Rao, A.M. Tanksale, M.S. Ghatge, V.V. Deshpande, Molecular and biotechnological aspects of microbial proteases, Microbiology and molecular biology reviews 62(3) (1998) 597-635.
[6] U. Eckhard, E. Schönauer, H. Brandstetter, Structural basis for activity regulation and substrate preference of clostridial collagenases G, H, and T, Journal of Biological Chemistry 288(28) (2013) 20184-20194.
[7] N.D. Rawlings, A.J. Barrett, A. Bateman, MEROPS: the peptidase database, Nucleic acids research (2009) gkp971.
[8] O. Matsushita, A. Okabe, Clostridial hydrolytic enzymes degrading extracellular components, Toxicon 39(11) (2001) 1769-1780.
[9] P. Ducka, U. Eckhard, E. Schönauer, S. Kofler, G. Gottschalk, H. Brandstetter, D. Nüss, A universal strategy for high-yield production of soluble and functional clostridial collagenases in E. coli, Applied microbiology and biotechnology 83(6) (2009) 1055-1065.
[10] K. Watanabe, Collagenolytic proteases from bacteria, Applied microbiology and biotechnology 63(5) (2004) 520-526.
[11] S.F. Altschul, T.L. Madden, A.A. Schäffer, J. Zhang, Z. Zhang, W. Miller, D.J. Lipman, Gapped BLAST and PSI-BLAST: a new generation of protein database search programs, Nucleic acids research 25(17) (1997) 3389-3402.
[12] S.F. Altschul, J.C. Wootton, E.M. Gertz, R. Agarwala, A. Morgulis, A.A. Schäffer, Y.K. Yu, Protein database searches using compositionally adjusted substitution matrices, The FEBS journal 272(20) (2005) 5101-5109.
[13] M.P. Styczynski, K.L. Jensen, I. Rigoutsos, G. Stephanopoulos, BLOSUM62 miscalculations improve search performance, Nature biotechnology 26(3) (2008) 274-275.
[14] B. Webb, A. Sali, Protein structure modeling with MODELLER, Protein Structure Prediction (2014) 1-15.
[15] R.L. Dunbrack, Rotamer Libraries in the 21 st Century, Current opinion in structural biology 12(4) (2002) 431-440.
[16] T.J. Dolinsky, P. Czodrowski, H. Li, J.E. Nielsen, J.H. Jensen, G. Klebe, N.A. Baker, PDB2PQR: expanding and upgrading automated preparation of biomolecular structures for molecular simulations, Nucleic acids research 35(suppl 2) (2007) W522-W525.
[17] M. Biasini, S. Bienert, A. Waterhouse, K. Arnold, G. Studer, T. Schmidt, F. Kiefer, T.G. Cassarino, M. Bertoni, L. Bordoli, SWISS-MODEL: modelling protein tertiary and quaternary structure using evolutionary information, Nucleic acids research (2014) gku340.
[18] S.C. Lovell, I.W. Davis, W.B. Arendall, P.I. de Bakker, J.M. Word, M.G. Prisant, J.S. Richardson, D.C. Richardson, Structure validation by Cα geometry: φ, ψ and Cβ deviation, Proteins: Structure, Function, and Bioinformatics 50(3) (2003) 437-450.
[19] R.A. Laskowski, M.W. MacArthur, D.S. Moss, J.M. Thornton, PROCHECK: a program to check the stereochemical quality of protein structures, Journal of applied crystallography 26(2) (1993) 283-291.

[20] C. Colovos, T.O. Yeates, Verification of protein structures: patterns of nonbonded atomic interactions, Protein science 2(9) (1993) 1511-1519.
[21] D. Eisenberg, R. Lüthy, J.U. Bowie, [20] VERIFY3D: Assessment of protein models with three-dimensional profiles, Methods in enzymology 277 (1997) 396-404.
[22] P. Benkert, S.C. Tosatto, D. Schomburg, QMEAN: A comprehensive scoring function for model quality assessment, Proteins: Structure, Function, and Bioinformatics 71(1) (2008) 261-277.
[23] J. Shen, W. Zhang, H. Fang, R. Perkins, W. Tong, H. Hong, Homology modeling, molecular docking, and molecular dynamics simulations elucidated α-fetoprotein binding modes, BMC bioinformatics 14(14) (2013) S6.
[24] G.M. Morris, R. Huey, W. Lindstrom, M.F. Sanner, R.K. Belew, D.S. Goodsell, A.J. Olson, AutoDock4 and AutoDockTools4: Automated docking with selective receptor flexibility, Journal of computational chemistry 30(16) (2009) 2785-2791.
[25] R. Huey, G.M. Morris, A.J. Olson, D.S. Goodsell, A semiempirical free energy force field with charge-based desolvation, Journal of computational chemistry 28(6) (2007) 1145-1152.
[26] A. Scozzafava, C.T. Supuran, Protease inhibitors–Part 5. Alkyl/arylsulfonyl-and arylsulfonylureido-/arylureido-glycine hydroxamate inhibitors of Clostridium histolyticum collagenase, European journal of medicinal chemistry 35(3) (2000) 299-307.
[27] Y. Zhang, Y. Fu, S. Zhou, L. Kang, C. Li, A straightforward ninhydrin-based method for collagenase activity and inhibitor screening of collagenase using spectrophotometry, Analytical biochemistry 437(1) (2013) 46-48.
[28] R. Bauer, J.J. Wilson, S.T.L. Philominathan, D. Davis, O. Matsushita, J. Sakon, Structural comparison of ColH and ColG collagen-binding domains from Clostridium histolyticum, Journal of bacteriology 195(2) (2013) 318-327.
[29] K. Kopka, H.J. Breyholz, S. Wagner, M.P. Law, B. Riemann, S. Schröer, M. Trub, B. Guilbert, B. Levkau, O. Schober, Synthesis and preliminary biological evaluation of new radioiodinated MMP inhibitors for imaging MMP activity in vivo, Nuclear medicine and biology 31(2) (2004) 257-267.

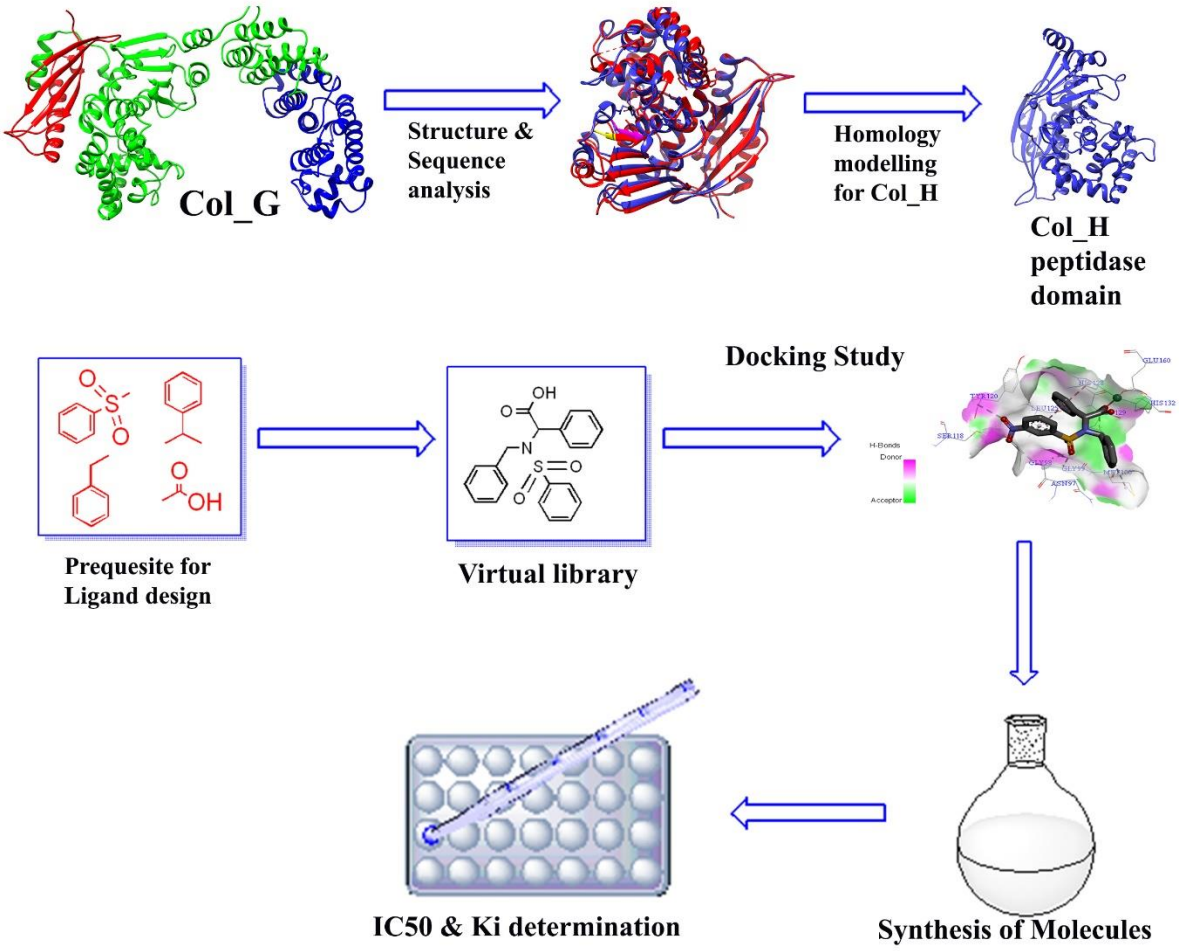

Fig. 1. Structure-based approach for development of Collagenase inhibitors. The structure and sequence of Clostridium collagenase Col_G and Col_H were compared showing high similarity with aspartate switch in Col_H as point of difference. The homology model for Col_H (open form after binding to inhibitor) was developed. The compounds were virtually screened by docking and synthesized. The IC_{50} of the compounds were experimentally determined through gelatin-ninhydrin assay and followed by determination of Ki of compound 5b.

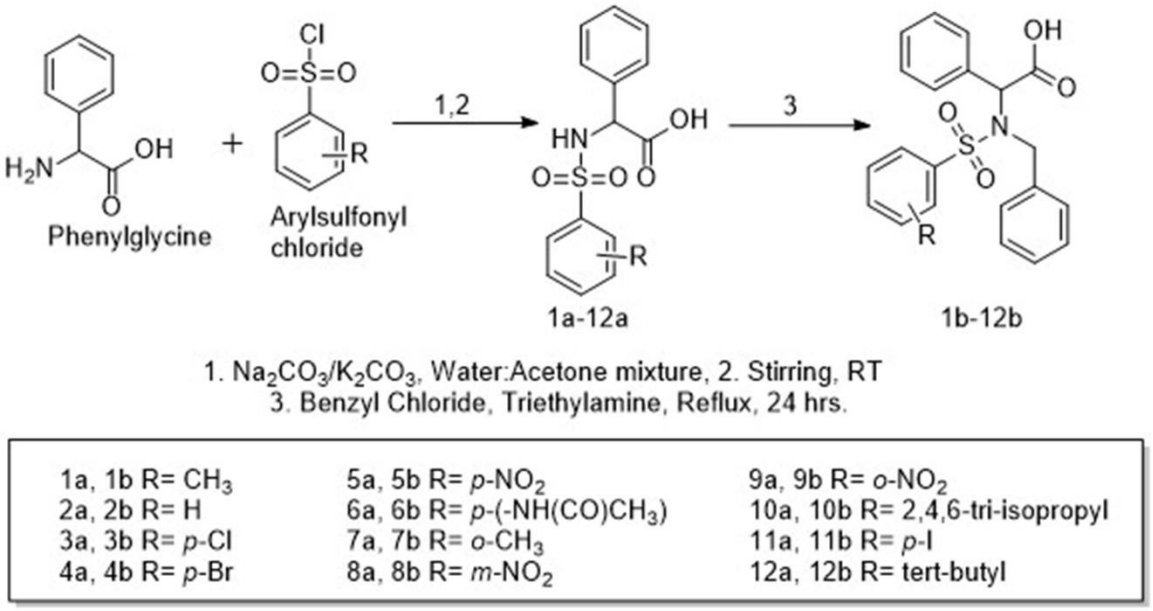

Fig. 2. Schemetic represenation of synthesis of *N-benzyl-arylsulfonyl-phenylglycine* (1b-12b) compounds.

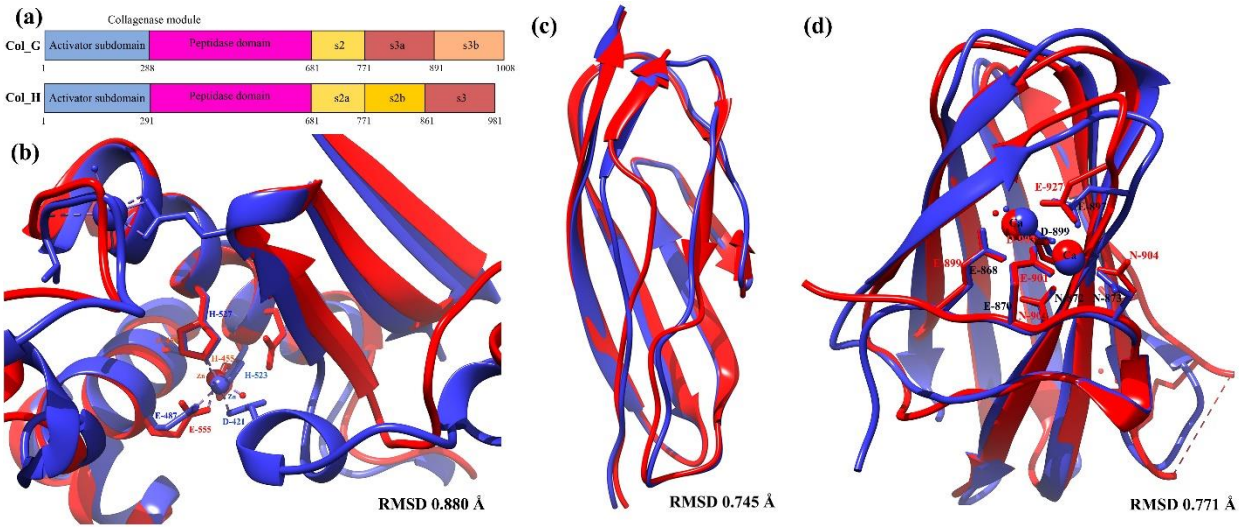

Fig. 3. (a) Structural comparision of Col_G and Col_H, (b) Structural superimposition of peptidase domain of Col_G:2Y50(red) and Col_H:4AR1(blue), (c) Structural superimposition of PKD of PKD s2 of Col_G:4AQO(red) and s2a of Col_H:4U6T (blue), (d) Structural superimposition of CBD s3b of Col_G:4HPK(red) and s3 of Col_H:3JQW(blue).

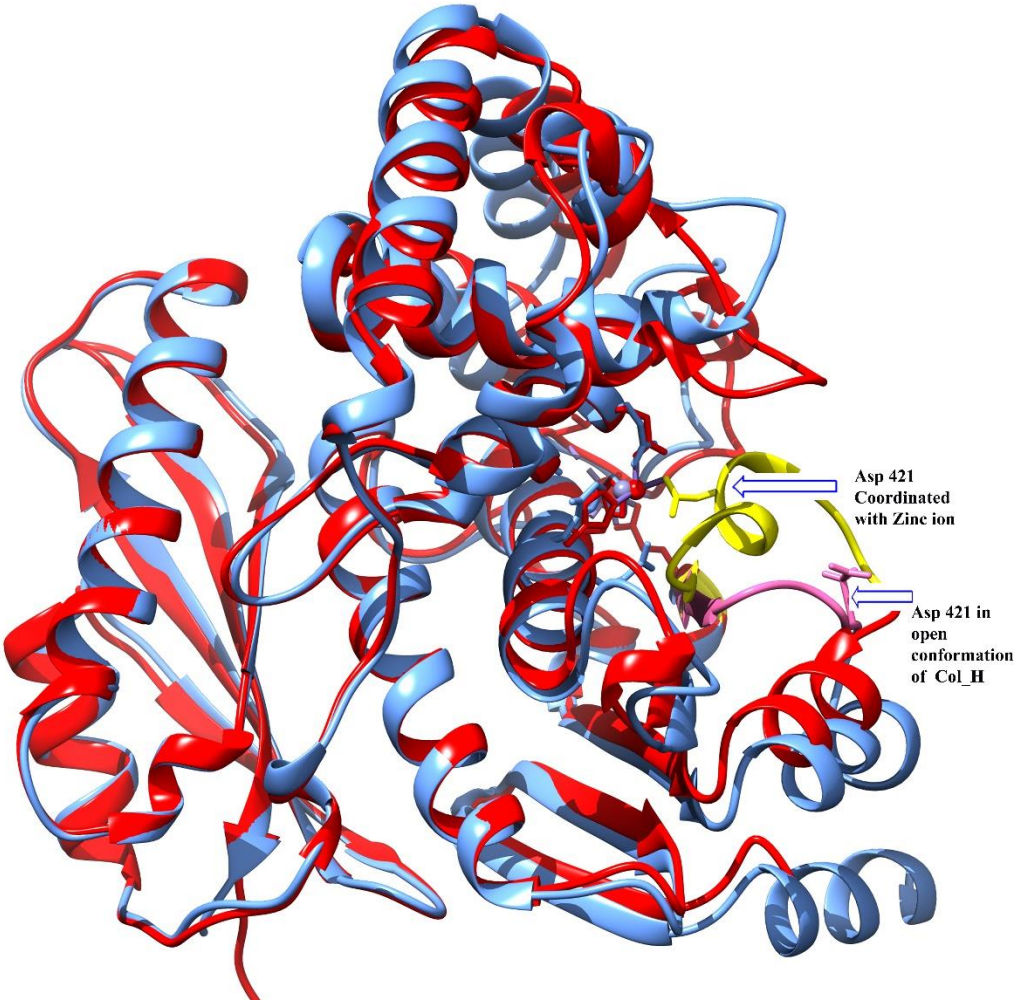

Fig. 4. Superimposition of Col_H peptidase 4AR1(red) and homology model(blue) showing displaced Asp 421(aspartate switch) leading to open conformation of Col_H in the developed homology model.

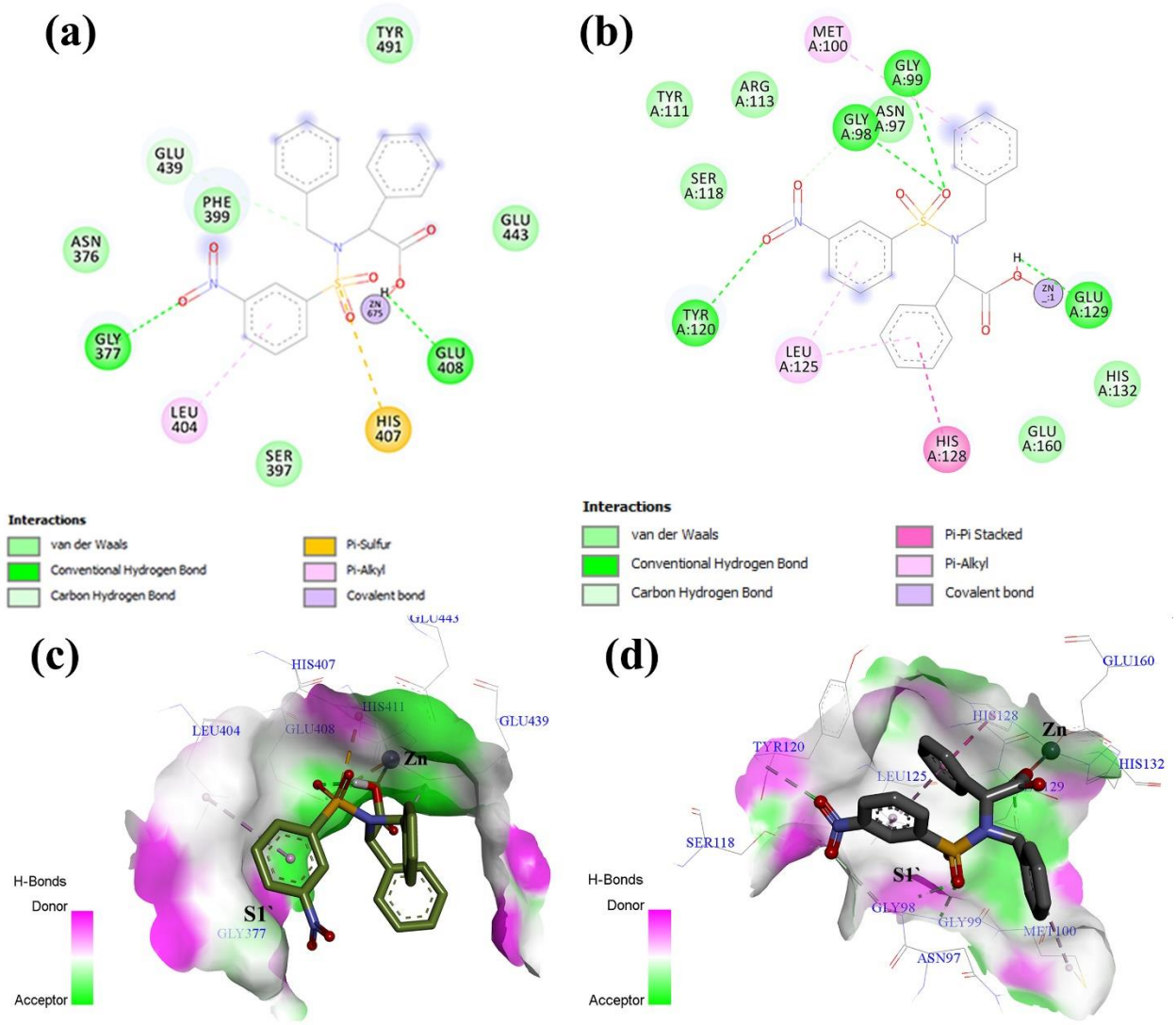

Fig. 5. (a & b) 2D-Docking interaction of compound 8b with Col_G(PDB id- 2Y50) and Col_H(PMDB id- PM0081035) respectively. (c & d) 3D-Docking interaction of compound 8b with Col_G(PDB id- 2Y50) and Col_H(PMDB id- PM0081035) respectively.

Table 1 Ramachandran quality parameter for homology model using RAMPAGE and PROCHECK.

Model	**Package**	**Ramachandran Plot Quality (%)**		
		Favoured	Allowed	Outlier
PMDB id-PM0081035	RAMPAGE	96.4	3.4	0.3
	PROCHECK	93.2	6.3	0.6

Table 2 Molecular docking results of designed compounds(1b-12b) with Col_G(PDB id- 2Y50)

Compound_id	**Binding energy (Kcal/mole)**	**Hydrogen bond**	**Interaction with Zinc**
1b	-7.64	1b:OH - GLU408:OE2(2.34 Å)	1b:O - Zn675(1.72 Å)
2b	-7.66	2b:OH - GLU408:OE2(1.66 Å)	2b:O - Zn675(1.52 Å)
3b	-6.28	GLY377:NH - 3b:O(2.26 Å) GLY378:NH - 3b:O(2.13 Å) 3b:OH - GLU439:OE2(1.97 Å)	Zn675 - GLU408:OE2(3.39 Å)
4b	-5.62	4b:OH - GLU408:OE2(1.78 Å)	No
5b	-7.51	SER397:OH -5b:O(2.03 Å) ARG392:NH - 5b:O(2.89 Å) 5b:COOH - GLU129:OE2(1.77 Å)	5b:O - Zn675(1.72 Å)
6b	-7.57	ASN492:HD22 - 6b:O(2.28 Å) 6b:H - GLU408:OE2(2.03 Å) 6b:H - GLU443:OE2(3.0 Å)	6b:O - Zn675(2.28 Å)
7b	-7.49	7b:H - GLU408:OE2(2.09 Å)	7b:O - Zn675(2.28 Å)
8b	-8.29	GLY377:NH - 8b:O(2.0 Å) 8b:H - GLU408:OE2(2.06 Å)	8b:O - Zn675(1.63 Å)
9b	-7.78	GLY377:NH - 9b:O(2.81 Å) GLY378:NH - 9b:O(2.44 Å) 9b:H - GLU439:OE1(2.15 Å)	9b:O - Zn675(1.52 Å)
10b	-5.73	10b:H - GLU408:OE2(1.90 Å)	10b:O - Zn675(1.90 Å)
11b	-8.02	11b:H - GLU408:OE2(1.5 Å)	11b:O - Zn675(1.56 Å)
12b	-8.13	12b:H - GLU408:OE2(1.74 Å)	12b:O - Zn675(1.76 Å)

Table 3 Molecular docking results of designed compounds(1b-12b) with Col_H(PMDB id-PM0081035)

Compound_id	Binding energy (Kcal/mole)	Hydrogen bond	Interaction with Zinc
1b	-6.95	1b:H - GLU129:OE2(2.22 Å)	1b:O - Zn675(1.72 Å)
2b	-6.59	2b:H - GLU129:OE2(1.93 Å)	2b:O - Zn675(1.57 Å)
3b	-6.13	GLY98:NH - 3b:O(2.20 Å) GLY99:NH - 3b:O(2.49 Å) 3b:H - GLU129:OE2(1.72 Å)	3b:O - Zn675(1.73 Å)
4b	-6.49	4b:H - GLU129:OE2(1.72 Å)	4b:O - Zn675(1.79 Å)
5b	-6.58	SER118:HG -5b:O(2.03 Å) TYR111:HH - 5b:O(2.82 Å) ARG113:HE - 5b:O(2.89 Å) 5b:COOH - GLU129:OE2(1.77 Å)	5b:O - Zn675(1.52 Å)
6b	-6.65	GLY98:NH - 6b:O(2.01 Å) GLY99:NH - 6b:O(2.79 Å	6b:O - Zn675(1.69 Å)
7b	-6.86	7b:H - GLU129:OE2(1.85 Å) GLY98:NH - 7b:O(2.29 Å) GLY99:NH - 7b:O(2.82 Å	7b:O - Zn675(1.73 Å)
8b	-7.97	GLY98:NH - 8b:O(2.07 Å) GLY99:NH - 8b:O(2.29 Å) TYR120:NH -8b:O(3.03 Å) 8b:H - GLU129:OE2(1.77 Å)	8b:O - Zn675(1.74 Å)
9b	-7.47	GLY98:NH - 9b:O(1.90 Å) GLY99:NH - 9b:O(2.23 Å) 9b:H - GLU129:OE1(1.76 Å)	9b:O - Zn675(1.72 Å)
10b	-6.18	10b:H - GLU129:OE2(1.96 Å)	10b:O - Zn675(1.70 Å)
11b	-7.31	11b:H - GLU129:OE2(1.92 Å)	11b:O - Zn675(1.70 Å)
12b	-7.19	12b:H - GLU129:OE2(1.74 Å)	12b:O - Zn675(1.60 Å)

Table 4 IC_{50} of compounds(1b-12b) against *Clostridium* Collagenase.

Compound_id	IC_{50}(μM)
1b	62.44 ± 0.064
2b	56.62 ± 0.028
3b	29.61 ± 0.025
4b	48.6 ± 0.18
5b	24.34 ± 0.40
6b	31.4 ± 0.040
7b	36.47 ± 0.033
8b	24.11 ± 0.030
9b	32.11 ± 0.052
10b	70.09 ± 0.028
11b	28.39 ± 0.25
12b	70.09 ± 0.034
1,10 Phenanthroline	28.28 ± 0.035